

noticeable. It seems reasonable to assume that contributions by incident f -waves are negligible in the energy range covered, in view of the small effect observed for d -waves. The absence of abrupt changes in the distributions observed indicates that probably several broad overlapping resonances in the compound nucleus participate in this reaction, as anticipated because of the high degree of excitation of the $B^{10}+D$

system. Due to the observed asymmetry, these levels must differ in parity.

It is a sincere pleasure to acknowledge the guidance and encouragement provided by Professor R. F. Humphreys throughout this investigation. The many informative discussions with Professor G. Breit on the interpretation of angular distribution data are appreciated.

PHYSICAL REVIEW

VOLUME 79, NUMBER 1

JULY 1, 1950

Low Energy Neutron Resonance Scattering and Absorption

S. P. HARRIS, C. O. MUEHLHAUSE, AND G. E. THOMAS

Argonne National Laboratory, Chicago, Illinois

(Received February 2, 1950)

Low energy neutron resonance absorption and scattering integrals have been measured, and resonance scattering fractions, Γ_n/Γ , have been determined for about thirty elements. Lightweight odd Z -even N and even Z -odd N isotopes are shown to have similar resonance phenomena. Correlations of level density and scattering fraction with atomic weight and nuclear type are presented.

I. INTRODUCTION

STRONG resonance absorption of slow neutrons has been observed for many elements since the discovery of neutron resonance phenomena by Fermi and others in 1936. The neutron spectrum of energies greater than thermal but less than 100 kev is usually referred to as the "epi-cadmium region," the "S-resonance region," or simply as the "resonance region." At these energies neutron scattering is almost entirely S -wave scattering. Though the existence of neutron resonance scattering was known experimentally and appreciated theoretically¹ as early as 1937, it was not until 1946 that Goldhaber^{2,3} showed that in the case of $^{25}\text{Mn}^{55}$ neutrons at resonance (~ 300 ev) were scattered much more frequently than they were absorbed. Since that time, additional nuclei have been found which possess primarily scattering resonances. Some of these are: (a) $^{27}\text{Co}^{59}$ (115 ev)⁴ 94 percent scattering; (b) $^{62}\text{Sm}^{152}$ (10 ev)⁵ 66 percent scattering; (c) $^{74}\text{W}^{186}$ (18 ev)^{6,7} 81 percent scattering.

The contribution to the total neutron cross section of scattering and absorption near resonance is given in the following simplified version of the Breit-Wigner

formula¹

$$\sigma_T(E) = \sigma_p + 4\pi\lambda_0^2 g \frac{\Gamma_n^2}{\Gamma^2} \frac{1}{1 + [(E - E_0)/(\Gamma/2)]^2} + 4\pi\lambda_0^2 g \frac{\Gamma_n \Gamma_\gamma}{\Gamma^2} \frac{1}{1 + [(E - E_0)/(\Gamma/2)]^2}$$

where: $\sigma_T(E)$ —total neutron cross section at energy E ; σ_p —potential scattering cross section; E_0 —energy of resonance; λ_0 —neutron wave-length (divided by 2π) at the resonance energy E_0 ; Γ_n —neutron resonance width at half-maximum; Γ_γ — γ -ray resonance width at half-maximum; Γ —total resonance width ($\Gamma_n + \Gamma_\gamma$) at half-maximum $g = \frac{1}{2}[1 \pm (1/2i + 1)]$ —statistical weight factor where " i " is the spin of the target (i.e., initial) nucleus. The second term in σ_T is the resonance scattering cross section, σ_{rs} , and the third term is the resonance absorption cross section, σ_{ra} .

The epi-cadmium neutron spectrum usually encountered (e.g., from a pile) is distributed in energy as $1/E$. An important measurable quantity, then, is the average epi-cadmium cross section for such a flux. In place of this, however, one usually considers a quantity proportional to the average epi-cadmium cross section, namely the resonance integral, Σ . This is defined as $\Sigma = \int \sigma_{res} dE/E$. Using the Breit-Wigner expressions for σ_{rs} and σ_{ra} , it can be readily shown that

$$\begin{aligned} \Sigma_s &= (\pi/2)(4\pi\lambda_0^2 g \Gamma/E_0) \Gamma_n^2/\Gamma^2 \quad \text{res. scatt. integral,} \\ \Sigma_a &= (\pi/2)(4\pi\lambda_0^2 g \Gamma/E_0) \Gamma_n \Gamma_\gamma/\Gamma^2 \quad \text{res. abs. integral,} \\ \Sigma_s + \Sigma_a &= (\pi/2)(4\pi\lambda_0^2 g \Gamma/E_0) \Gamma_n/\Gamma \quad \text{total res. integral,} \end{aligned}$$

¹ H. A. Bethe and G. Placzek, Phys. Rev. **51**, 450 (1937).

² M. Goldhaber and A. A. Yalow, Phys. Rev. **69**, 47(A) (1946).

³ N. H. Barbre and M. Goldhaber, Phys. Rev. **71**, 141(A) (1947).

⁴ Harris, Langsdorf, and Seidl, Phys. Rev. **72**, 866 (1947).

⁵ M. Goldhaber and A. W. Sunyar, Phys. Rev. **76**, 189(A) (1949).

⁶ M. Goldhaber and L. L. Lowry, Phys. Rev. **76**, 189(A) (1949).

⁷ S. P. Harris and C. D. Muehlhause, Phys. Rev. **76**, 189(A) (1949).

TABLE I. Flux ratio for 7-cm separation in rabbit.

Nucleus	Thermal ratio — <i>gth</i>	Resonance ratio		Fast neutron ratio — <i>gf</i>
		Activation energy (ev)	<i>gr</i>	
Al	1.38			
Cu	1.38	0.6 to 1	1.57	
In		1.44	1.56	
Au		4.8	1.54	
Co		115	1.56	
Mn	1.38	345	1.56	
P				1.79
Average	1.38	1.56		1.79

from which

$$\Sigma_s/(\Sigma_s + \Sigma_a) = \Gamma_n/\Gamma \quad \text{and} \quad \Sigma_a/(\Sigma_s + \Sigma_a) = \Gamma_\gamma/\Gamma.$$

These ratios represent the probability of resonance scattering and of absorption, respectively. The resonance integrals are important in themselves, however, since they relate the various resonance parameters. For example, knowing Γ_n/Γ and E_0 , it is possible to calculate $g\Gamma$ from either Σ_s or Σ_a .

It is the purpose of this paper to present measurements of Σ_s and Σ_a for a number of elements, and in addition to obtain average values of Γ_n/Γ . It will be demonstrated that, in general, resonance scattering is a prominent fraction of the total resonance integral.

II. DETERMINATION OF Σ_a

A. The Cadmium Ratio, Cd R

The neutron flux from the Argonne heavy water reactor is composed of two principal energy bands: thermal and epi-cadmium ($1/E$). The ratio of thermal absorption to epi-cadmium absorption for a given isotope in this flux can be determined by measuring the cadmium ratio. Since cadmium absorbs thermal neutrons exclusively, the ratio of absorption without cadmium to absorption with cadmium relates the thermal absorption cross section to the average epi-cadmium absorption cross section. Measurement of a cadmium ratio is usually accomplished by means of activation.

$$\text{Cd } R = \frac{\text{activation (no Cd)}}{\text{activation (with Cd)}} = 1 + \text{const. } \sigma_{tha}/\Sigma_a',$$

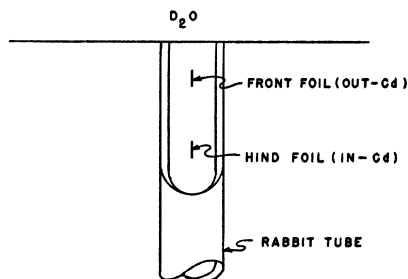


FIG. 1. Diagram of foil positions in rabbit flux.

TABLE II. Cadmium ratio for gold, indium, and boron in rabbit, port, and thimble fluxes.

Nucleus	Rabbit	Cadmium ratio (Cd-R)	
		Thimble	Port (beam)
B	~70		
In	3.26	2.44	2.31
Au	2.91	2.25	

or

$$\Sigma_a' = K[\sigma_{tha}/(\text{Cd } R - 1)]$$

$K = \text{constant (depending on flux only)}$

where σ_{tha} is the thermal activation cross section and Σ_a' is the resonance absorption integral plus any "1/V" absorption beyond the cadmium cut-off energy (~ 0.6 ev). With regard to this latter component of absorption, it should be noted that the thermal absorption cross section decreases with neutron energy as $1/E^{1/2}$. Since cadmium suddenly ceases to absorb neutrons at ~ 0.6 ev, some absorption or activation due to the thermal cross section is present even with a cadmium cover. This 1/V component of epi-cadmium absorption, $\Sigma_{1/v}$, is accounted for by writing

$$\Sigma_a' = \Sigma_a + \Sigma_{1/v}.$$

The proportionality constant, K , between thermal and resonance absorption is obtained by measuring the Cd R for a known resonance absorber such as gold, in which⁸ $\Sigma_a = 1296\text{b}$ and⁹ $\sigma_{tha} = 93\text{b}$, where b indicates "barns" ($1 \text{ barn} \equiv 10^{-24} \text{ cm}^2$). Then,

$$\Sigma_a' = (\text{Cd } R - 1)_{\text{Au}} \frac{\Sigma_a'_{\text{Au}}}{\sigma_{tha \text{ Au}}} \cdot \frac{\sigma_{tha}}{\text{Cd } R - 1} \equiv K \frac{\sigma_{tha}}{\text{Cd } R - 1}. \quad (1)$$

Therefore, by so comparing the Cd R of a substance with gold, and by knowing its thermal absorption cross section, Σ_a' can be evaluated. The advantage of this method is that only relative intensity measurements of the same activity are made. This can be done with high accuracy. Such a measurement of Σ_a' then depends on the more easily determined σ_{tha} . Measurements should be made with foils which are so thin that peak resonance absorption (i.e., at the maximum value of the resonance cross section) is a linear function of foil thickness.

It remains to be shown how the 1/V-component of epi-cadmium absorption is determined. This is obtained from a measurement of the Cd R for a pure 1/V-type absorber such as boron. In this case,

$$\Sigma_a' = \Sigma_{1/v} = K \frac{\sigma_{1/v}}{(\text{Cd } R - 1)_{1/v}} \equiv k\sigma_{1/v}$$

where $\sigma_{1/v}$ is the thermal absorption cross section of the 1/V absorber. Therefore, the proper resonance ab-

⁸ Best fit to Breit-Wigner formula using Columbia data by M. Goldhaber.

⁹ Argonne mechanical velocity selector data by A. Wattenberg.

TABLE III. Resonance absorption integrals.

Isotope	Cd-R	$\frac{\Sigma_a'}{\sigma_{tha}}$	σ_{tha} (barns)	Σ_a' (barns)	$\Sigma_{1/v}$ (barns)	Σ_a (barns)	Source of σ_{tha}	10^{24} nuclei per cm ² (isotopic)	Chemical form
¹¹ Na ²³	70.3	~0.4	0.52	~0.21	~0.21	~0	P	7.4×10 ⁻⁶	NaF
¹³ Al ²⁷	43.1	~0.65	0.22	~0.14	~0.09	~0.05	P	2.9×10 ⁻⁴	Al
¹⁵ P ³¹	63.8	~0.44	0.23	~0.10	~0.09	~0.01	S	3.1×10 ⁻⁴	P
²¹ Sc ⁴⁵	69.0	~0.4	31.6	~12.6	~12.6	~0	P	2.6×10 ⁻⁵	Sc ₂ O ₃
²³ V ⁵¹	70.6	~0.4	4.93	~2.0	~2.0	~0	P	2.1×10 ⁻⁵	V ₂ O ₅
²⁵ Mn ⁵⁵	35	~0.81	12.1	~9.8	~4.8	~5	P	6.5×10 ⁻⁵	Mn
²⁷ Co ⁵⁹	23.8	1.20	34.3	41.2	13.7	27.5	P	6.1×10 ⁻⁵	Co
²⁹ Cu ⁶³	30.8	0.92	3.62	3.35	1.45	1.90	P	1.4×10 ⁻⁴	Cu
²⁹ Cu ⁶⁵	30.5	0.93						6.0×10 ⁻⁵	Cu
³¹ Ga ⁶⁹	5.79	5.72	1.40	8.01	0.56	7.45	S	3.1×10 ⁻⁵	Ga ₂ O ₃
³¹ Ga ⁷¹	7.96	3.94	3.36	13.2	1.3	11.9	S	2.0×10 ⁻⁵	Ga ₂ O ₃
³³ As ⁷⁵	4.36	8.15	3.87	31.5	1.6	29.9	P	6.0×10 ⁻⁵	As
³⁵ Br ⁷⁹	3.25	12.2	10.9	133	4	129	S	1.0×10 ⁻⁵	PbBr ₂
³⁹ Y ⁸⁹	47.9	0.58	1.24	0.72	0.50	0.22	S	4.1×10 ⁻⁵	Y ₂ O ₃
⁴¹ Nb ⁹³	9.59	3.19	1.31	4.19	0.52	3.67	P	2.5×10 ⁻⁵	Nb ₂ O ₅
⁴⁵ Rh ¹⁰³	7.94	3.95	149	589	60	529	S	2.6×10 ⁻⁵	Rh
⁴⁷ Ag ¹⁰⁷	13.35	2.22	44.3	98.3	17.7	80.6	S	1.5×10 ⁻⁵	Ag
⁴⁷ Ag ¹⁰⁹	3.20	12.5	97.0	1213	39	1174	S	Zero extrapolation	Ag
⁴⁹ In ¹¹³	2.68	16.3	56.0	913	22	891	S	6.8×10 ⁻⁷	In
⁴⁹ In ¹¹⁵	3.26	12.1	196	2372	78	2294	S	1.5×10 ⁻⁶	In
⁵¹ Sb ¹²¹	2.27	21.6	6.8	147	3	144	S	1.7×10 ⁻⁵	Sb
⁵¹ Sb ¹²³	~1.55	~50	2.5	~125	1	~124	S	1.3×10 ⁻⁵	Sb
⁵³ I ¹²⁷	2.45	19.0	6.25	119	3	116	S	1.3×10 ⁻⁵	PbI ₂
⁵⁹ Pr ¹⁴¹	30.9	0.92	10.1	9.3	4.0	5.3	S	1.8×10 ⁻⁵	PrO ₂
⁶³ Sm ¹⁵²	3.43	11.3	138	1559	55	1504	S	4.1×10 ⁻⁶	Sm ₂ O ₃
⁶³ Eu ¹⁵¹	45.7	0.61	1380	842	552	290	S	8.3×10 ⁻⁶	Eu ₂ O ₃
⁷² Hf ¹⁸⁰	14.9	1.97	10.0	19.7	4.0	15.7	S	8.0×10 ⁻⁶	HfO ₂
⁷² Hf ¹⁸¹	~3.0	~14	~100	~1400	40	~1360	P	2.3×10 ⁻⁵	HfO ₂
⁷³ Ta ¹⁸¹	25.1	25.1	20.6	517	10	507	S	2.7×10 ⁻⁵	Ta
⁷⁴ W ¹⁸⁶	3.93	9.35	34.2	320	14	306	S	3.1×10 ⁻⁷	W
⁷⁵ Re ¹⁸⁵	3.61	10.5	101	1061	40	1021	S	6.6×10 ⁻⁶	Re
⁷⁵ Re ¹⁸⁷	8.50	3.65	75.3	275	30	245	S	1.1×10 ⁻⁵	Re
⁷⁷ Ir ¹⁹¹	9.37	3.27	1000	3270	400	2870	S	6.9×10 ⁻⁶	Ir
⁷⁷ Ir ¹⁹³	3.89	9.48	128	1213	51	1162	S	1.1×10 ⁻⁵	Ir
⁷⁹ Au ¹⁹⁷	2.91	14.35	93	1337	37	1296	Wattenberg	5.0×10 ⁻⁷	Au
⁸¹ Tl ²⁰³	3.59	10.6	~12	127	~5	122	P	3.0×10 ⁻⁵	Tl
⁸¹ Tl ²⁰⁵	7.12	4.48	~.17	.76	~.07	~.69	P	7.3×10 ⁻⁵	Tl

Note.—Key to "source of σ_{tha} ": P—pile (reference 10); S—Seren (reference 11).

sorption integral, Σ_a , is given by

$$\Sigma_a = \Sigma_a' - k\sigma_{tha}. \tag{2}$$

B. Energy and Space Distribution of the Flux

The so-called "rabbit flux" of the Argonne heavy water reactor was chosen as the most convenient neutron flux for making activation measurements. The rabbit consisted of a pneumatic tube which conducted a pair of samples to be bombarded into the pile at a position next to the heavy water tank, as illustrated in Fig. 1. One sample was covered with cadmium (in-Cd sample) while the other sample was not (out-Cd sample). Each sample pair was ejected after its proper time of bombardment. In-Cd and out-Cd samples were bombarded at the same time and were always separated 7 cm apart in the rabbit tube. This insured that (a) both samples received the same bombardment time at the same pile power, and (b) the neutron flux ratio (out-Cd to in-Cd) remained constant for all sample pairs.

Several experiments were performed to investigate the spacial distribution of the rabbit flux for various neutron energies.

(1) Pairs of thermal (i.e., $\sim 1/V$) absorber foils were activated 7 cm apart out of cadmium to determine the ratio of thermal neutron intensity for a 7-cm separation in the rabbit.

(2) Pairs of resonance absorber foils were activated 7 cm apart inside cadmium to determine this ratio for various energy resonance neutrons.

(3) Two phosphorus foils were activated 7 cm apart inside cadmium to determine this ratio for neutrons > 1 Mev energy.

These results are given in Table I from which it can be seen that *gr* (flux ratio for resonance neutrons) is constant, i.e., is independent of energy. This is the only

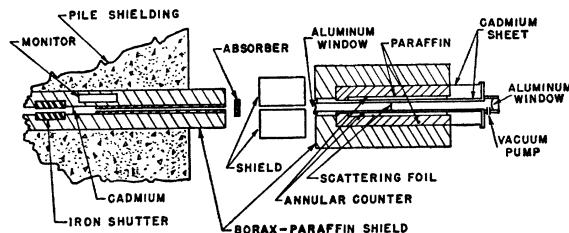


FIG. 2. Schematic diagram of scattering apparatus.

TABLE IV. Resonance scattering integrals.

Isotope	$\sigma_{\text{epi-Cd}}$ (barns)	σ_P (barns)	σ_{th} (barns)	Σ_a' (barns)	E_0 ev	Σ_s (barns)	Source of σ_P	10^{24} nuclei per cm ²	Chemical form
⁶ C ¹²	4.60	4.60					<i>H</i>	4.5×10^{-3}	C
¹¹ Na ²³	7.6	4.4		27	~3000	~51	<i>H'</i>	1.4×10^{-4}	NaF
¹³ Al ²⁷	1.80	1.46		2.9	>40 kev	~9	<i>H</i>	7.7×10^{-3}	Al
²¹ Sc ⁴⁵	16.0		12.8	27	10^3 - 10^4	~60		8.7×10^{-5}	Sc ₂ O ₃
²³ V ⁵¹	16.2	5.0		94	~2700	~190	<i>H'</i>	5.0×10^{-4}	V
²⁴ Cr ⁵³	17.7		8.4	78	~4200	166		7.5×10^{-5}	Cr ₂ ⁵³ O ₃
		Corrected							
²⁵ Mn ⁵⁵	35.4	3.8		265	345, 2400	425	<i>H</i>	7.4×10^{-5}	Mn
²⁷ Co ⁵⁹	42.5	7.3		296	115	435	<i>H</i>	9.9×10^{-5}	Co
²⁹ Cu ⁶³	9.1	6.7		20	~ 10^3	~35	<i>H</i>	2.4×10^{-4}	Cu
³⁰ Zn ⁶⁷	36		7	244	480	410		7.3×10^{-5}	Zn ⁶⁷ O
³¹ Ga ⁶⁹	17.0	8.1		75	10^2 - 10^3	~126	<i>F</i>	2.2×10^{-4}	Ga
³³ As ⁷⁵	12.2	6.9		45	10^2 - 10^3	~76	<i>H</i>	8.0×10^{-5}	As
³⁵ Br ⁸¹	8.8	7.9		7.6	~10	~9.2	<i>H</i>	2.6×10^{-3}	CBr ₄
³⁹ Y ⁸⁹	5.1		4.0	9.2	—	—		5.3×10^{-5}	Y ₂ O ₃
⁴¹ Nb ⁹³	7.7	7.2		4.2	—	—	<i>H</i>	6.4×10^{-4}	Nb
⁴⁵ Rh ¹⁰³	6.3		3.6	23	1.28	24		1.8×10^{-4}	Rh
⁴⁷ Ag ¹⁰⁷	7.4	6.8		5.0	~15	~6.2	<i>F</i>	4.9×10^{-5}	Ag ¹⁰⁷ O
⁴⁷ Ag ¹⁰⁹	12.4	7.7		39.5	5.2	46	<i>F</i>	4.7×10^{-5}	Ag ¹⁰⁹ O
⁵¹ Sb ¹¹¹	8.91	5.35		29.9	~10	~36.3	<i>H</i>	4.9×10^{-5}	Sb
⁵³ I ¹²⁷	10.0	5.15		40.7	20-30	~53	<i>H</i>	4.6×10^{-5}	PbI ₂
⁵⁷ La ¹³⁹	10.1	9.1		8.4	—	—	<i>F</i>	3.7×10^{-5}	La ₂ O ₃
⁵⁹ Pr ¹⁴¹	15.0		8.0	59	~ 10^2 (?)	~72		3.6×10^{-5}	PrO ₂
⁶² Sm ¹⁴⁷	102		23	664	10	806		3.4×10^{-5}	Sm ₂ O ₃
⁶³ Eu ¹⁵¹	34.1		30.1	34	~10	~41		3.3×10^{-5}	Eu ₂ O ₃
⁶⁴ Gd ¹⁵⁷	24		26					3.3×10^{-5}	Gd ₂ O ₃
⁷² Hf ¹⁷⁸	53.8		26.0	234	7.7	279		2.8×10^{-5}	HfO ₂
⁷³ Ta ¹⁸¹	17.8	10.7		59.6	4.0	69	<i>H</i>	5.0×10^{-5}	Ta
⁷⁴ W ¹⁸⁶	149		23	1058	~15	~1330		2.6×10^{-5}	W ¹⁸⁶ O ₃
⁷⁵ Re ¹⁸⁷	22.2	15.2		58.8	2.3	64.6	<i>H</i>	3.2×10^{-5}	Re
⁷⁹ Au ¹⁹⁷	29.6	10.8		158	4.8, >345	~210	<i>H</i>	7.6×10^{-6}	Au
⁸¹ Tl ²⁰⁵	14.7	11.7		25.2	260	39.8	<i>H</i>	3.0×10^{-4}	Tl

Note.—Key to "source of σ_P ": *H*—reference 13; *H'*—unpublished; *F*—thick filter (see Section III-C).

quantity of actual importance in calculating the Cd *R* flux is evidently distributed as $1/E$ since:

front foil (nearest tank) \equiv out-Cd foil,
hind foil (farthest from tank) \equiv in-Cd foil.

The hind foil activity had therefore to be multiplied by the factor 1.56.

A second point of interest was to determine if the epi-cadmium neutron energy distribution of the rabbit flux was actually of the form $1/E$. This was accomplished by comparing the ratio of $(Cd R-1)$ for two substances (1) and (2) measured in the rabbit flux and in the thimble flux (central vertical tube of the pile), which latter flux was known to vary as $1/E$. If both fluxes have the same epi-cadmium energy distribution, then:

$$[(Cd R-1)_1 / (Cd R-1)_2] = [\sigma_{\text{th}a1} \Sigma_{a2}' / \sigma_{\text{th}a2} \Sigma_{a1}'].$$

This is to say that if two neutron fluxes differ only in the relative magnitudes of their thermal and epi-cadmium neutron intensities, the above quantity is a constant characteristic of the materials (1) and (2), and not of the fluxes. Table II gives data on gold and indium pertinent to the above point and, in addition, lists similar data for indium measured in a neutron beam from one of the reactor ports. The rabbit epi-cadmium

flux is evidently distributed as $1/E$ since:

$$\left\{ \frac{(Cd R-1)_{\text{In}}}{(Cd R-1)_{\text{Au}}} \right\}_{\text{Rabbit}} = 1.18$$

and

$$\left\{ \frac{(Cd R-1)_{\text{In}}}{(Cd R-1)_{\text{Au}}} \right\}_{\text{Thimble}} = 1.15.$$

C. Calibration

Calculation of the constants "*K*" and "*k*" in formulas (1) and (2) is now possible from the data given in Table III.

First, from the light element data of Table III, $(Cd R)_{1/v} \approx 70$. This is taken from the data on ¹¹Na²², ²¹Sc⁴⁵, and ²³V⁵¹. These isotopes have no known important neutron capture levels near zero energy which could cause any epi-cadmium neutron absorption other than $1/V$ absorption. Therefore:

$$k = K / (Cd R)_{1/v} = K / 69.$$

Second, from the measured cadmium ratio of gold (2.91):

$$K = (\Sigma_{a' \text{Au}} / \sigma_{\text{th}a \text{Au}}) (Cd R-1)_{\text{Au}} = [(1296 + 93k) / 93] 1.91.$$

These taken together yield $K = 27.4$ and $k = 0.4$. That is,

$$\Sigma_{a'} = 27.4 [\sigma_{\text{th}a} / (Cd R-1)] \quad \text{and} \quad \Sigma_{1/v} = 0.4 \sigma_{\text{th}a}.$$

$(Cd R)_{1/v}$ is of considerable significance when compared directly with another $Cd R$ in the same neutron flux, since

$$\begin{aligned} (Cd R)_{1/v} > Cd R \rightarrow E_0 > 0.6 \text{ ev,} \\ (Cd R)_{1/v} < Cd R \rightarrow E_0 < 0.6 \text{ ev.} \end{aligned}$$

$(Cd R)_{1/v}$ therefore represents the critical case of non-resonance. If $\Sigma_a < 0$, the most prominent neutron absorption resonance has an energy < 0.6 ev (cadmium cut-off energy). An example of this is ${}_{66}\text{Dy}^{164}$ where $Cd R \approx 215$.

D. Preparation of Samples

Samples were usually of high purity. It was important that they be dry. This insured the absence of hydrogen in the samples, which if present would cause neutron moderation and consequent extra activation via thermal absorption of the in-Cd sample. Other impurities were less important since an activation technique permitted isolation of the period being studied. Unless in elemental foil form, all samples were fixed to a 1-cm² area and 1-mil thick puron (electrolytic iron) foil, which material becomes only slightly active under neutron bombardment. The powders (metals or oxides) were fixed by the application of one drop of thinned zapon (an organic adhesive), which substance when dry introduced a negligible amount of hydrogen into the sample and produced no measurable activity of its own. Such samples were usually < 5.0 mg/cm². Strong resonance absorbers ($Cd R < 5$) were either evaporated on the puron to thickness ~ 0.2 mg/cm² or zaponed to the puron to thicknesses ~ 1.0 mg/cm².

In preparing samples care was also taken to maintain equal thicknesses for the out-Cd and in-Cd samples. This was necessary to minimize (1) slight non-linear neutron resonance absorption, and (2) different radiation detection efficiencies.

E. Activation Measurements

Sample activities were either measured on a Geiger counter or in a no-window air ionization chamber. This latter instrument was especially useful in cases where (1) $Cd R > 50$, since a greater intensity range was available with the ionization chamber than with the Geiger counter, and (2) the activity consisted largely of electrons too soft to penetrate a Geiger counter window.

When several activities had to be observed over a long period of time, activity standards such as uranium were employed. In short, when all the usual precautions were taken, these operations yielded results with a probable error of ~ 2 percent. Therefore, if the thermal absorption cross section was uncertain to only ~ 2 percent, the calculated resonance absorption integral, Σ_a , would be most limited by the five percent uncertainty in the gold standard. There were many cases, however, in which the thermal absorption cross section had an uncertainty of ~ 20 percent. This difficulty was at

times avoided by the use of the pile neutron absorption cross section, σ_{pile} .¹⁰ This is the neutron absorption cross section for a material placed in the center of the reactor (thimble). Such a pile cross section is made up principally of two parts, (a) the thermal absorption cross section, and (b) some fraction of the epi-cadmium absorption cross section (i.e., integral). In the Argonne heavy water reactor, σ_{pile} is given by $\sigma_{pile} = \sigma_{tha} + 0.054\Sigma_a$. When σ_{pile} had been measured with sufficiently thin samples, it could be combined with the value for Σ_a'/σ_{tha} (obtained from the $Cd R$ measurement) to evaluate both Σ_a and σ_{tha} . When this was not the case, σ_{tha} was obtained from the neutron activation cross-section measurements of Seren¹¹ and others at Argonne. The source of σ_{tha} is indicated in column 8 of Table III.

$Cd R$ of hafnium was determined by a different method¹² which will be described only briefly in this paper. The principal absorption in hafnium does not lead to an assigned activity.^{12a} However, $Cd R$ (Hf) was determined using the neutron beam from one of the pile ports and two anthracene scintillation γ -ray counters in coincidence. The capture γ -ray intensity from a thin Hf O₂ foil with and without cadmium in the beam was measured. This was then standardized with the $Cd R$ for indium given in Table II.

F. Results of Σ_a

Table III lists values of $Cd R$, Σ_a'/σ_{tha} , σ_{tha} , Σ_a' , $\Sigma_{1/v}$, Σ_a , sample thickness, and the source of σ_{tha} . Though the error in Σ_a'/σ_{tha} is less than five percent, other values are in general uncertain to 10 or 20 percent. Strong capture resonances are prominent in the region above zirconium but less than tin and in the region above lanthanum but less than lead.

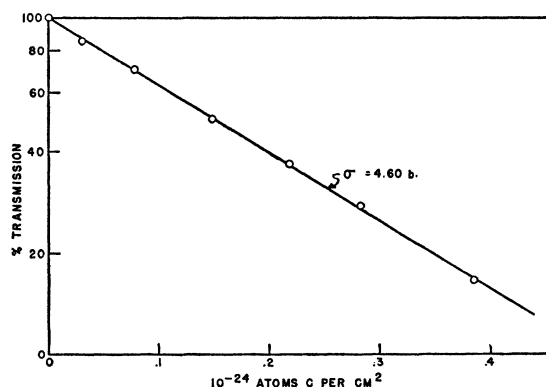


FIG. 3. Semilog plot of carbon transmission curve of carbon-detected epi-cadmium neutrons.

¹⁰ Harris, Muehlhause, Rasmussen, Schroeder, and Thomas (to be published).

¹¹ Seren, Friendlander, and Turkel, Phys. Rev. 72, 888 (1947).

¹² C. O. Muehlhause, Phys. Rev. (to be published).

^{12a} The unassigned 19-sec. Hf period may be an isomer of the stable isotope that results from the principal absorption in hafnium. There is evidence of this from the fact that $Cd R$ (19-sec. Hf) ≈ 3.1 and $Cd R$ (Hf) ≈ 3.0 .

III. DETERMINATION OF Σ_s

A. Apparatus

The apparatus has been described in a previous paper.^{4,13} Briefly, it consists of a 4π -annular proportional neutron counter filled with enriched BF_3 and surrounded by a paraffin reflector-moderator and shield. An evacuated hole through the center of the counter conducts a collimated beam of cadmium-filtered neutrons from the Argonne heavy water reactor. These neutrons give rise to a counting rate only when a scattering foil (termed the detector) is placed in the center of this tube transverse to the neutron beam. Provision is made for monitoring the neutron flux by simultaneously counting the pulses from a fission counter imbedded in the collimator. The chamber-circuit deadtime is 15 μsec . The equipment is illustrated schematically in Fig. 2.

B. Flux Conditions

Though the epi-cadmium neutron beam from the reactor is distributed in energy as $1/E$, the counting rate using a flat detector foil (i.e., one in which the scattering cross section is constant) falls off more rapidly with neutron energy than $1/E$. This results from the fact that though the paraffin reflector markedly increases the sensitivity of the boron counter at high energies, the efficiency still decreases with increasing neutron energy. Experimentally, the counter sensitivity has been shown to decrease as $\log E$ (logarithm of neutron energy)¹⁴ falling off by a factor of ~ 8.0 between 0.5 ev (cadmium cut-off energy for the beam) and 1.5 Mev (mean fission energy). One can express the counter sensitivity at energy E , $S(E)$, relative to the counter sensitivity at cadmium cut-off energy, $S(\text{Cd})$, by:

$$[S(E)/S(\text{Cd})] \simeq 1 - 0.0587 \log 2E.$$

This means that a scattering resonance integral measured with this counter would be too small. Simple analysis will show that the proper value of a scattering integral, Σ_s , is greater than the measured value, Σ_s' , by the ratio of the counter sensitivity at cadmium cut-off energy to the counter sensitivity at the reso-

nance energy, E_0 . That is

$$\Sigma_s = [S(\text{Cd})/S(E_0)] \Sigma_s'. \quad (3)$$

C. Theory of Measurement

When a thin detector foil (i.e., scattering foil) is placed in the center of the annular chamber, the counting rate due to neutrons scattered by the foil will be proportional to both its potential scattering cross section, σ_p , and to its effective resonance scattering integral, Σ_s' . The average scattering cross section of the foil, $\sigma_{\text{epi-Cd}}$, for epi-cadmium neutrons can be determined by comparing the neutron counting rate from the foil with that from a flat detector such as carbon: $\sigma_{\text{epi-Cd}} = \sigma_C(N/N_c)(n_c/n)$ where N and N_c are the counting rates of the foil and carbon, respectively, n and n_c are the atoms per cm^2 of the foil and carbon, respectively, and σ_C is the constant carbon scattering cross section.

If a given material possesses no resonance scattering (i.e., $\Sigma_s = 0$), then the average epi-cadmium scattering cross section, $\sigma_{\text{epi-Cd}}$, is just equal to the potential scattering cross section, σ_p . It is reasonable to expect, and a simple analysis will show, that the effective resonance scattering integral, Σ_s' , is proportional to the difference between $\sigma_{\text{epi-Cd}}$ and σ_p . The sensitivity function determines the constant of proportionality to be about 8.4. That is

$$\Sigma_s' = 8.4(\sigma_{\text{epi-Cd}} - \sigma_p). \quad (4)$$

Therefore, the measurement of $\sigma_{\text{epi-Cd}}$ and σ_p will yield the effective resonance scattering integral, Σ_s' , which can be corrected to the proper scattering resonance integral, Σ_s , when the resonance energy, E_0 is known.

Three principal sources or methods for determining the potential or off-resonance scattering cross section, σ_p , are available. (1) Neutrons near the resonance energy, E_0 , are removed from the neutron beam with a thick filter of the material being studied. This filter is placed in the neutron beam outside the counter shield. A comparison of counting rates with carbon is again made which will now yield σ_p . (2) Numerous values of σ_p are available from the work of Hibdon and Muehlhause.¹³ Those relevant to this paper have been used. (3) Lacking both of the above sources of σ_p , the thermal scattering cross section can be used in place of σ_p .

In the above discussion, carbon is assumed to be a flat detector (i.e., σ_C is independent of the energy). This is admittedly not quite true over the entire energy range. At energies up to about 5000 ev, our measurements indicate $\sigma_C = 4.72b$. However, the neutron spectrum extends to energies at which σ_C is as low as $2.0b$. For practical purposes the average epi-cadmium cross section of carbon serves very well. This is determined by measuring the total cross section of carbon using a carbon detector. Figure 3 is a semilog plot of the epi-cadmium neutron transmission of carbon using a carbon detector. The transmission curve is a straight line

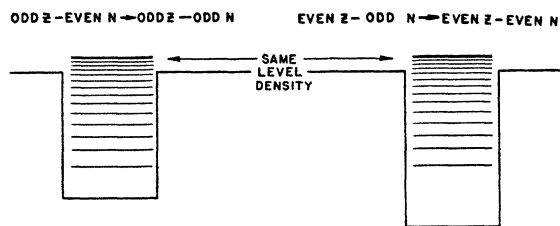


FIG. 4. Compound nuclei resulting from a neutron plus an odd Z -even N and an even Z -odd N nucleus.

¹³ C. T. Hibdon and C. O. Muehlhause, Phys. Rev. **76**, 100 (1949).

¹⁴ R. W. Gurney (private communication).

TABLE V. Resonance scattering fraction: Γ_n/Γ .

Isotope	E_0 ev	Σ_a	Σ_s	Σ_T	Γ_n/Γ	Comments
$^{13}\text{Al}^{27}$	>40 kev	0.05	~9	~9	>0.99	
$^{25}\text{Mn}^{55}$	345, 2400	~5	425	430	~0.99	$J_1=3$
$^{27}\text{Co}^{59}$	115	27.5	435	463	0.94	
$^{29}\text{Cu}^{63}$	10^2 - 10^4	1.90	~35	~37	0.95	
$^{31}\text{Ga}^{69}$	10^2 - 10^3	7.45	~126	~133	~0.95	
$^{33}\text{As}^{75}$	10^2 - 10^3	29.9	~76	~106	~0.72	
$^{45}\text{Rh}^{103}$	1.28	529	24	553	0.043	
$^{47}\text{Ag}^{107}$	~15	80.6	~6.2	~86.8	~0.071	
$^{47}\text{Ag}^{109}$	5.1	1174	46	1220	0.038	
$^{51}\text{Sb}^{121}$	~10	136	~36.3	~172	~0.21	
$^{53}\text{I}^{127}$	20-30	116	~53	~169	~0.31	
$^{59}\text{Pr}^{141}$	~10(?)	5.3	72	~77	~0.94	
$^{62}\text{Sm}^{152}$	10	1504	2975	4479	0.66	
$^{72}\text{Hf}^{181}$	<10	1360	279	1639	0.17	$\Gamma_n \sim \Gamma_\gamma$ at 7.7 ev.
$^{73}\text{Ta}^{181}$	4.0	507	69	576	0.12	
$^{74}\text{W}^{186}$	~15	306	~1340	~1646	~0.81	
$^{75}\text{Re}^{187}$	2.3	531	64.6	596	0.11	
$^{79}\text{Au}^{197}$	4.8, >345	1296	~210	1506	0.14	$\Gamma_n/\Gamma > 0.9$ for $E_0 > 345$ ev Probably TI^{203}
$^{81}\text{Tl}^{203}$	260	36.5	39.8	76.3	.52	

whose slope yields the proper epi-cadmium total cross section. Since carbon is very nearly a pure scatterer (i.e., no absorption), this value of $4.60b$ can be used for σ_C .

D. Preparation of Samples

Whenever possible, the elemental foil form was used for detectors. Otherwise dry powders (metals, oxides, fluorides) were fixed to 0.5-mil aluminum foils. The fixing was accomplished as described in Section II-D. Again it was important to insure a minimum presence of hydrogen. In this case, the presence of hydrogen caused an extra counting rate due to its high scattering cross section ($\sim 20b$). The backing was accounted for by measuring the counting rate from a 0.5-mil aluminum foil with the same amount of zapon attached.

E. Counting Technique

Counting rate measurements were always made with and without the detector foil in place. In the case of powders fixed to aluminum, the background was considered to be that from an aluminum foil having the same number of zapon drops as were used to fix the powders. The scattering due to oxygen or fluorine was subtracted according to their known¹³ potential scattering cross sections

$$\sigma_p(\text{oxygen}) = 4.12b, \quad \sigma_p(\text{fluorine}) = 3.62b.$$

All counting rates were monitored by the fission counter and corrected for deadtime losses. These measurements had a probable error of about two percent.

F. Results on Σ_s

Table IV lists the data on $\sigma_{\text{epi-Cd}}$, σ_p or the thermal scattering cross section σ_{ths} , Σ_s' , and, when possible, Σ_s . In addition, the source of σ_p is indicated. These results have a probable error of 10 to 20 percent. This large uncertainty arises from two sources. First, the

sensitivity function, $S(E)$, which determines both the correction factor in Eq. (3) and the scale factor in Eq. (4) is known only to about 10 percent. Second, in many cases σ_p is known only to about 10 percent since it is not always measurable by any of the procedures employed (Section III-C and reference 13). For example, the general depression in the scattering cross section of $^{25}\text{Mn}^{55}$ ($E_0=345$ and ~ 2400 ev)¹⁵ below 50 ev is due to the destructive interference of resonance and potential scattering. This is operative even in the thermal region, as is evidenced by the fact that manganese exhibits a negative scattering phase at thermal energies.¹⁶ An asymptotic cross section (i.e., using thick filters (Section III-C) or a thermal scattering cross section ($\sigma_{\text{ths}}=2.6b$) is, therefore, different from the proper value of σ_p .

In the case of hafnium, the large resonance scattering observed is due principally^{16a} to a resonance level at 7.7 ev.¹⁷

Σ_s' for gold is too large to be accounted for by the 4.8-ev resonance level.¹⁸ It is probably due to a prominent scattering resonance >345 ev, since strong resonance overlapping between gold and manganese has been reported.¹³

The large resonance scattering in $^{11}\text{Na}^{23}$ indicates a low energy scattering resonance. Details of this resonance at ~ 3000 ev have been reported.¹⁹

Observation of Table IV reveals 10 elements or isotopes out of 31 in which $\Sigma_s > 100b$. Sizable resonance scattering at low energies appears to be associated with

¹⁵ High speed Argonne resonance time-of-flight velocity selector data by W. Selove.

¹⁶ E. Fermi and L. Marshall, Phys. Rev. **71**, 666 (1947).

^{16a} A boron transmission curve of hafnium scattered neutrons indicated a resonance energy of ~ 7.5 ev. See reference 13 for details of method.

¹⁷ Havens, Wu, Rainwater, and Meaker, Phys. Rev. **71**, 165 (1947), Zr curve.

¹⁸ Reference 17, Au curve.

¹⁹ Hibdon, Muehlhause, Selove, and Woolf, Phys. Rev. **77**, 730 (1950).

odd Z -even N and even Z -odd N lightweight isotopes.²⁰ In the medium heavy region, certain even Z -even N isotopes have very large scattering resonance integrals (e.g., ${}_{62}\text{Sm}^{152}$, ${}_{72}\text{Hf}^{\text{even}}$, ${}_{74}\text{W}^{186}$). The heavy elements may also exhibit sizable resonance scattering for resonance levels ~ 100 ev (e.g., ${}_{79}\text{Au}^{197}$, ${}_{81}\text{Tl}^{\text{odd}}$).

In the light element region (less than 50 neutrons), many unreported even Z -even N isotopes were examined and found to have no observable resonance scattering. From this we may conclude that the nearest level to zero energy is greater than 10 kev. On the other hand, in two cases^{21,22} of Oak Ridge separated even Z -odd N isotopes^{23,24} (${}_{24}\text{Cr}^{53}$ at ~ 4200 ev, ${}_{30}\text{Zn}^{67}$ at 480 ev) strong resonance scattering was found which accounted for all of the observed resonance scattering of the normal element. Evidently the odd Z -even N and even Z -odd N isotopes have comparable level densities in their respective compound nuclei near the neutron binding energy. This situation is depicted in Fig. 4. An odd Z -even N isotope forms an odd Z -odd N compound nucleus with a shallow well whose first excited state is not far off ground. An even Z -odd N isotope forms an even Z -even N isotope with a deep well whose first excited state is far above the ground level. It is not unreasonable to expect such nuclei to have about the same level spacing near binding (i.e., near zero energy for the incoming neutron). Such a picture is in agreement with observations on neutron induced radioactivity (e.g., Mattauch's rules²⁵).

It remains to be shown why the even Z -even N isotopes have a greater level separation near binding in

the compound nucleus. In the medium heavy region, the even Z -even N isotopes display level spacings of the order of 10 to 100 times greater than their odd Z or odd N neighbors. Therefore, if this level spacing factor is maintained in the lightweight region, no resonance levels < 10 kev would be expected for even Z -even N isotopes.

One further observation not complete in Table IV should be made. No significant resonance scattering or absorption exists for ${}_{40}\text{Zr}^{90}$ (50 neutrons), ${}_{50}\text{Sn}$ (50 protons), ${}_{57}\text{La}^{139}$ (82 neutrons), or ${}_{83}\text{Bi}^{209}$ (126 neutrons). These elements are at magic number positions.^{26,27} It is furthermore true that neutron resonance levels are more widely separated in the region following a magic number. The closed shells perhaps account for (a) the appearance of strong capture resonances (i.e., high level density) soon after the element zirconium, (b) the disappearance of dense levels near tin (50 protons), (c) the reappearance of dense levels in the rare earth region after lanthanum (82 neutrons), and (d) the second disappearance of dense levels near lead (82 protons) and bismuth (126 neutrons).

IV. THE SCATTERING FRACTION, Γ_n/Γ

Table V re-lists the measured values of Σ_s and Σ_a for cases in which the scattering fraction Γ_n/Γ is calculated. For most of the isotopes studied $\Gamma_n/\Gamma > 0.1$. The light odd Z -even N and even Z -odd N are such that $\Gamma_n/\Gamma \sim 0.9$. The scattering fraction decreases with increasing atomic weight principally because resonance levels appear which are nearer zero neutron energy. It appears that resonance scattering and absorption are comparable for resonance energies of about 10 to 50 ev. Below 10 ev, capture is the principal resonance component. Above 50 ev, scattering is the principal resonance component. Many of the features indicated in Section III are also revealed in Table V.

²⁰ S. P. Harris, and A. S. Langsdorf, Phys. Rev. **74**, 1216(A) (1948).

²¹ Preliminary results on the odd isotope of germanium (73) indicate that the prominent (see reference 22) resonance at ~ 95 ev is primarily a scattering resonance and due to ${}_{32}\text{Ge}^{73}$.

²² Wu, Rainwater, and Havens, Phys. Rev. **71**, 174 (1947).

²³ W. W. Havens and L. J. Rainwater, Phys. Rev. **75**, 1296(A) (1949).

²⁴ Goldsmith, Ibser, and Feld, Rev. Mod. Phys. **19**, 259 (1947).

²⁵ J. Mattauch, *Kernphysikalische Tabellen* (Verlag. Julius Springer, Berlin, 1942).

²⁶ M. G. Mayer, Phys. Rev. **74**, 235 (1948).

²⁷ M. G. Mayer, Phys. Rev. **75**, 1969 (1949).